Evaluation of Parameter Variations of Equivalent Circuit Model of Lithium-ion Battery under Different SOH Conditions

Zhiyong Xia, *Student Member, IEEE*, and Jaber A. Abu Qahouq, *Senior Member, IEEE*

The University of Alabama
Department of Electrical and Computer Engineering
Tuscaloosa, Alabama 35487, USA

Abstract—**This paper studies the patterns of equivalent circuit model (ECM) parameter variations under different state-of-health (SOH) conditions for lithium-ion battery. An ECM is constructed in this paper to characterize the ageing behavior of battery by fitting ECM to experimentally measured EIS data within the frequency range from 0.01 Hz to 7.928 kHz. The experimentally measured EIS and SOH data are obtained from an accelerated ageing experiment of lithium-ion battery conducted in the laboratory. The comparison between the EIS data generated from the constructed ECM and experimentally measured EIS data validates the constructed ECM. The variations of the parameters of the ECM as a function of the changes in the SOH of the battery showed that as the battery's health deteriorates overtime, the value of series resistor of the ECM increases and the values of the capacitance components of CPE of the ECM decrease. The presented model and its results can provide a way to estimate or co-estimate the SOH of the battery.**

Keywords—Battery, lithium-ion, battery management system (BMS), capacity, impedance, electrochemical impedance spectroscopy (EIS), equivalent circuit model (ECM), state-of-charge (SOC), state-of-health (SOH), electric vehicle.

I. INTRODUCTION

Over the past decade, the market of electric vehicles (EVs) has been growing [1-21]. Lithium-ion battery energy storage systems have been widely adopted in the EVs [1-16]. Battery management systems (BMSs) are usually designed to achieve high energy efficiency and high safety specifications [1-8]. State-of-health (SOH) estimation is desired to be included in BMS to monitor the health status of battery system and improve reliability and safety performance of battery system [12-17].

Electrochemical impedance spectroscopy (EIS) is an effective analytical technique which can help to gain insight on the electrochemical mechanisms of battery [10-13]. It is a useful indicator of internal state of battery. In the literature, the EIS is utilized to estimate state-of-charge (SOC), SOH, remaining useful life (RUL), internal temperature of battery and perform fault diagnosis [9-11]. Several online EIS measurement methods are presented in the literature [8-12]. This facilitates the real time applications of EIS based estimation algorithms.

Equivalent circuit model (ECM) is a common approach to characterize the dynamic behaviors of battery [12-18]. It is usually utilized to fit the experimentally measured EIS data under different battery operation conditions, such as different SOC, SOH, and ambient temperature values. The parameter variation patterns of ECM under these different operation conditions are analyzed and utilized to develop different estimation methods of internal state of battery. Compared with directly utilizing EIS data to estimate the internal state of battery, the ECM method uses a few parameters to store EIS data for internal state estimation [18]. This saves memory resources in microcontroller or microprocessor, which is preferable for resource-limited real-time applications.

In this paper, an ECM is constructed to fit the experimentally measured EIS data of lithium-ion battery. The parameter variation patterns of developed ECM are investigated and evaluated when the value of SOH of battery changes. From the obtained experiment results, it is observed that with the increasing of health deterioration level of lithium-ion battery, the value of series resistor of the ECM increases and the values of capacitance of CPE components of the ECM decreases. The presented ECM model and its results can provide an way to estimate or co-estimate the SOH of the battery.

The remaining part of this paper is organized as follows: Section II discusses the developed ECM, Section III presents the preliminary experiment results for the ECM parameter variation patterns, and the conclusion is given in Section IV.

II. ECM FOR LITHIUM-ION BATTERY

Fig. 1 shows the diagram of the constructed ECM for lithium-ion battery in this paper. The description for each component/element in this model is listed in Table I. The constant phase element (CPE) results from the double layer effect occurring between the anode electrode and the cathode electrode, i.e. the ions moving back and forth between the anode electrode and the cathode electrode through the electrolyte [19]. The CPE is used to characterize the behavior of the non-ideal or imperfect capacitor. The impedance for this capacitor is given by Equation (1) [22].

$$Z = \frac{1}{Y_o} \times \frac{1}{(j\omega)^\alpha} \qquad (1)$$

Where Y_o represents the capacitance of CPE, and it is usually a constant, ω is the radian frequency, and the exponent α is a constant whose value is usually less than 1. For the ideal capacitor, the value of exponent α is equal to 1. The Warburg impedance W is used to represent the diffusion process occurring inside the battery. It appears like a straight line with 45° angle in the EIS curve. The Warburg impedance can be considered as a special case of CPE where the exponent α is equal to 0.5 [22]. $V_{oc(SOC)}$ is the open circuit voltage of battery (i.e. when the battery is unloaded and at equilibrium state). It varies with the value of state-of-charge (SOC) of battery.
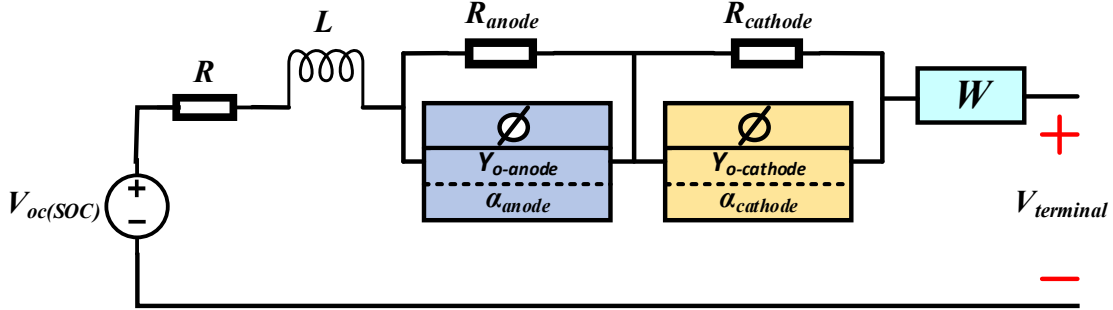

Fig. 1. The diagram of the constructed ECM for Lithium-ion battery in this paper.

Table I. The circuit components of the constructed ECM in this paper.

Model component	Description
$V_{oc(SOC)}$	Open circuit voltage of battery. It varies with the SOC value of battery.
R	Series resistor which mainly models the resistance of electrolyte and current collector of battery.
L	Inductive component which models the porous nature of battery electrodes [12].
R_{anode}	Resistance parameter to characterize the behavior of double layer effect occurring close to anode electrode. It is responsible for one of two semi-circles in the EIS [21].
$Y_{o-anode}$	Capacitance parameter of CPE for anode electrode. It is responsible for one of two semi-circles in the EIS.
α_{anode}	Fractional phase element coefficient of CPE for anode electrode.
$R_{cathode}$	Resistance parameter to characterize the behavior of double layer effect occurring close to cathode electrode. It is responsible for one of two semi-circles in the EIS.
$Y_{o-cathode}$	Capacitance parameter of CPE for cathode electrode. It is responsible for one of two semi-circles in the EIS.
$\alpha_{cathode}$	Fractional phase element coefficient of CPE for cathode electrode.
W	Warburg impedance which models diffusion process occurring in low frequency region of EIS.

Simplex algorithm [23] is the adopted model fitting algorithm to obtain the parameter values of the constructed ECM. It is a linear programming algorithm which is used here to find the values of different circuit component parameters (i.e. R, L, R_{anode}, $Y_{o-anode}$, α_{anode}, $R_{cathode}$, $Y_{o-cathode}$, $\alpha_{cathode}$, W for the ECM in this paper) to have minimum error between the EIS data generated from the ECM and the experimentally measured EIS data.
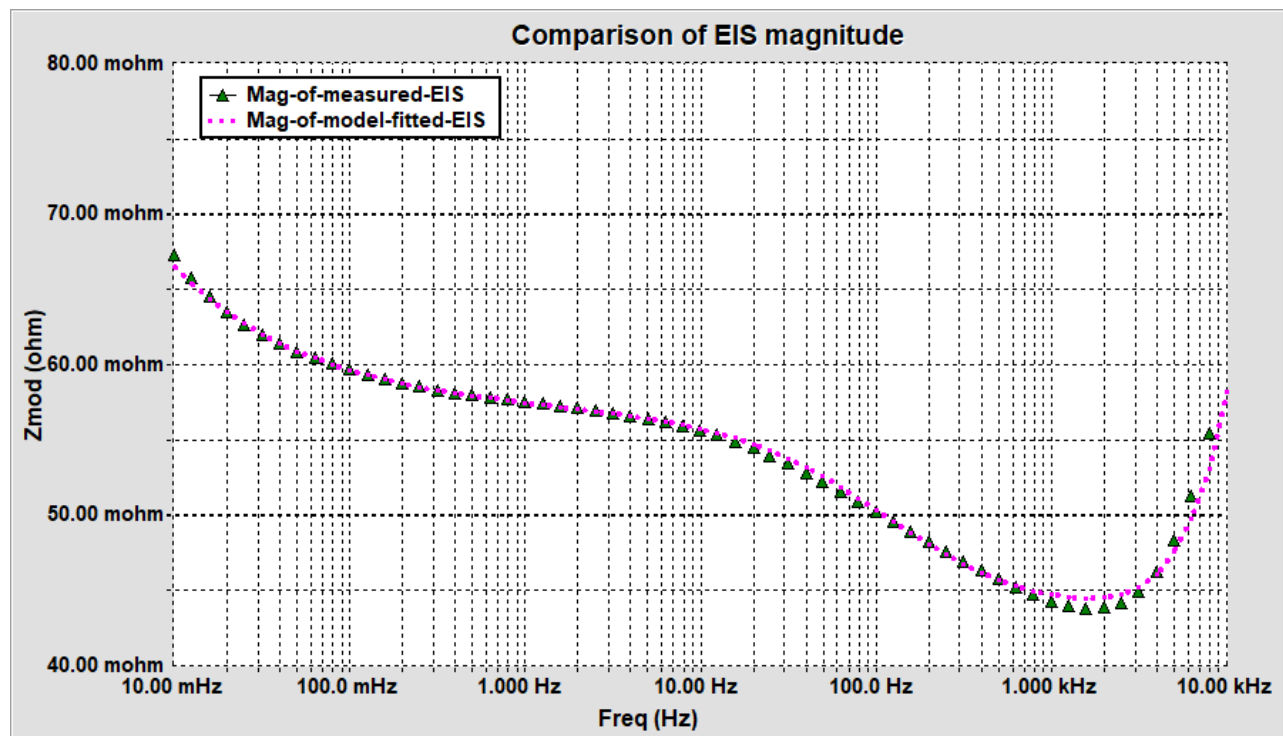
Fig. 2 shows plots that compare the experimentally measured EIS data with the model fitted EIS data within frequency range from 0.01 Hz to 7.928 kHz. These plots are generated using Gamry Echem Analyst software [24]. The experimentally measured EIS data in this paper is obtained using Gamry Instruments Interface 5000E™ [25]. It can be observed that the EIS plot of the presented ECM matches well with the experimentally measured EIS plot. This indicates the presented ECM can characterize the behaviors of the battery.

III. Preliminary Experimental Results

The battery used in this paper is Tenergy 18650-2600 and its main specifications are listed in Table II [26]. The protocol used to age lithium-ion battery in this paper is: 1 C (i.e. 2.6 A) constant discharge current, 2.7 V discharge cut-off voltage, 1 C constant charging current, 4.2 V termination voltage for constant current charging, 0.05 A termination current for constant voltage charging, and one full discharge operation and one full charge operation are counted as one complete ageing cycle. The EIS measurement is performed after 30 minutes rest time once a charging operation is completed, i.e. when the state-of-charge (SOC) of battery is 100% and the battery reaches the thermal equilibrium from the charging operation. The EIS measurement is repeated every 30 ageing cycles.

The lithium-ion battery investigated in this paper are aged for 150 cycles, which resulted in 10.9% capacity fading. The definition of SOH is based on the capacity fading concept given by Equation (2).

$$SOH = \frac{Q_{now}}{Q_{nominal}} \times 100\% = (1 - \text{Capacity fading}) \times 100\% \quad (2)$$

1520

(a)
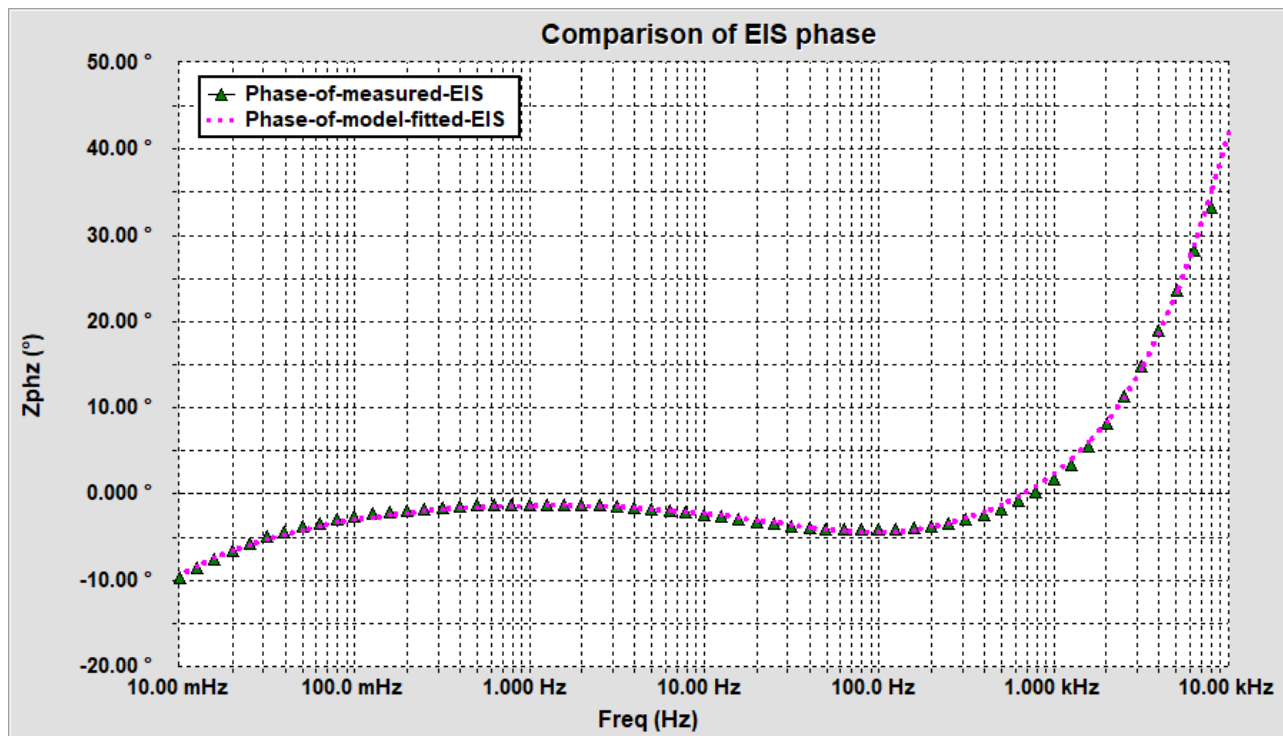
(b)

Fig. 2. Comparison between experimentally measured EIS data and ECM model fitted EIS data within frequency range from 0.01 Hz to 7.928 kHz: (a) EIS magnitude and (b) EIS phase. This figure is generated using Gamry Echem Analyst software [24] and the experimentally measured EIS data is obtained using Gamry Instruments Interface 5000E™ [25].

1521

Where Q_{now} is the total amount of charges the battery can currently supply and $Q_{nominal}$ is the nominal capacity specified in the manufacturer's document or can be experimentally measured when the battery is new by Coulomb counting the fully discharged charges. The range of the value of SOH is between 0 and 1 or 0% and 100%. The smaller the value of SOH is, the more the battery health is deteriorated.

Type	Lithium-ion cell
Model	Tenergy 30005-0
Nominal capacity	2600 mAh
20% capacity fading	~@300 cycles
Nominal voltage	3.7 V
Maximum discharge current	2 C (5200 mA)

Table III. The values of SOH under different ageing cycles.

Cycle	0	30	60	90	120	150
SOH	1	0.964	0.943	0.921	0.909	0.891

The number of charges which the battery supplies (i.e. the value of Q_{now}) is calculated during discharging operation by using Coulomb counting method. This information is utilized to calculate the SOH of the aged lithium-ion battery for different ageing cycles as given by Equation (2). The results are shown in Table III. It can be observed that when the battery goes through more ageing cycles, the value of SOH decreases (which is expected).

Fig. 3 shows parameter variation patterns of the constructed ECM under different SOH conditions. It can be noted that the value of R increases when the value of SOH decreases. This helps to explain why the power losses of battery increases when battery degrades. The capacitance values of CPE components, i.e. $Y_{o-anode}$ and $Y_{o-cathode}$, decrease with the decreasing of SOH. This helps to explain why the energy storage capability of the battery decreases when the health status of battery degrades. The battery can essentially be assumed to have a similar behavior as a capacitor that operates as the energy storage component, and its energy storage capability will decrease when the battery health deteriorates. The inductance value L is very small with magnitude level of 0.1 μH (it can be assumed to be constant during the ageing process). For other circuit components of the constructed ECM, no clear variation patterns are observed based on the ageing data collected from the accelerated ageing experiment conducted in this paper.
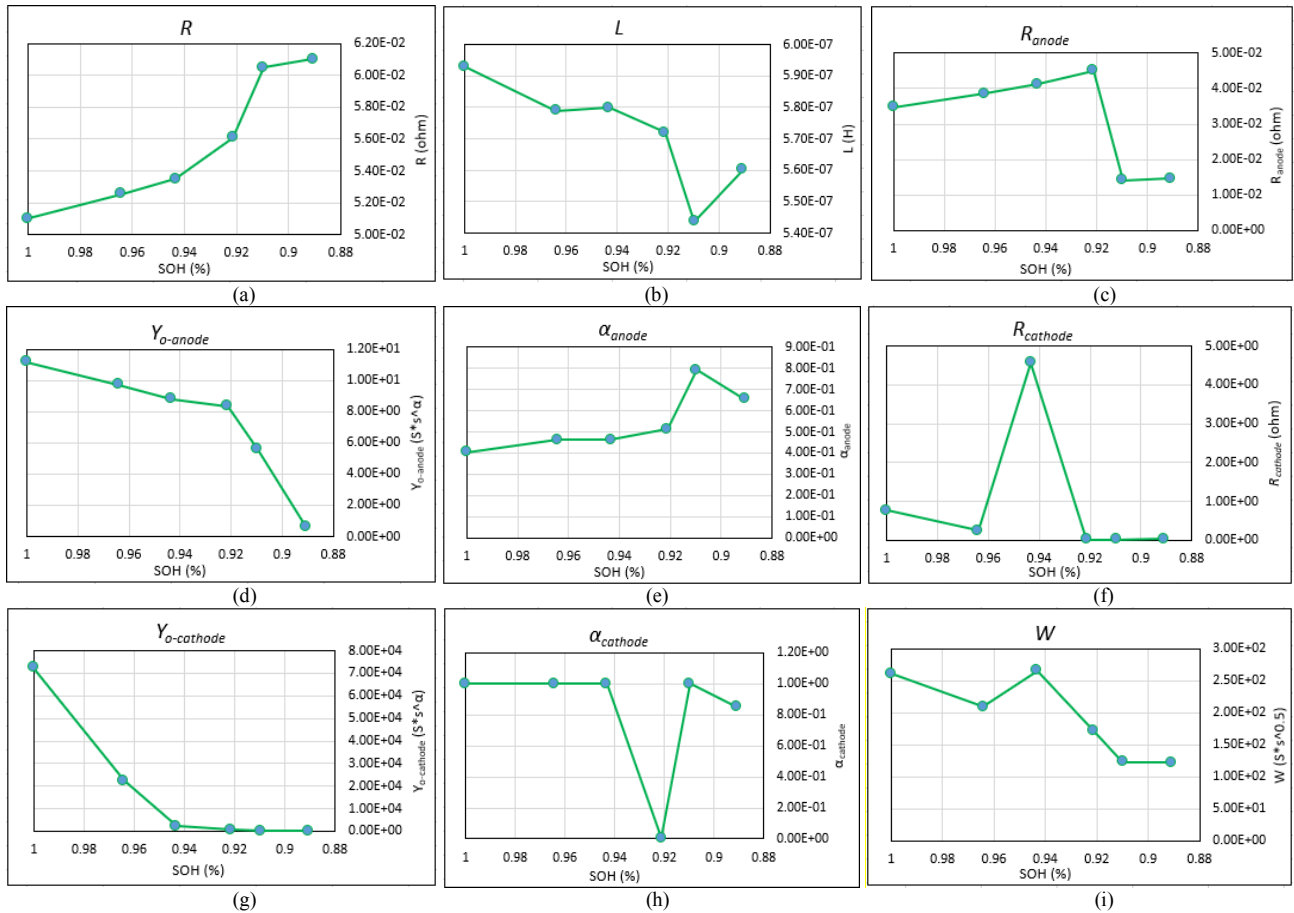

Fig. 3. Parameter variations of the constructed ECM under different SOH conditions.

IV. CONCLUSION

In this paper, an ECM is constructed to characterize the aging behaviors of lithium-ion battery by fitting the model to the experimentally measured EIS data as the battery ages (as the battery health degrades). The parameter variations of the ECM are evaluated and analyzed under different SOH conditions. The experiment results show that over the accelerated ageing process, the value of series resistor of the ECM increases and the values of capacitance of CPE components of the ECM decreases. These variation patterns help to understand the degradation characteristics of lithium-ion battery and in developing SOH estimation methods. Future work includes but is not limited to accelerated ageing experiments with different ageing conditions, such as different depth-of-discharging, discharging current, and temperature values.

REFERENCES

[1] H. R. Eichi, U. Ojha, F. Baronti, and M. Y. Chow, "Battery management system: an overview of its application in the smart grid and electric vehicles," *IEEE Industrial Electronics Magazine*, vol. 7, no. 2, pp. 4-16, June 2013.

[2] J. A. Abu Qahouq and Y. Cao, "Control scheme and power electronics architecture for a wirelessly distributed and enabled battery energy storage system," *Energies*, vol. 11, no. 7, July 2018.

[3] W. Huang and J. A. Abu Qahouq. "Energy Sharing Control Scheme for State-of-Charge Balancing of Battery Energy Storage System," *IEEE Trans. Ind. Electron.*, vol. 62, no. 5, pp. 2764-2776, May 2015.

[4] Yuan Cao and Jaber Abu Qahouq, "Evaluation of bi-directional single-inductor multi-input battery system with state-of-charge balancing control," *IET Power Electronics Journal*, Volume 11, Issue 13, pp: 2140 - 2150, 2018.

[5] W. Huang and J. Abu Qahouq, "Small-signal modeling and controller design of energy sharing controlled distributed battery system", *Simulation Modelling Practice and Theory*, vol. 77, pp. 1-19, September 2017.

[6] Y. Gao, S. Li, W. Dong, and B. Lu, "Decoupled AC/DC Power Flow Strategy for Multiterminal HVDC Systems," *International Journal of Emerging Electric Power Systems*, vol. 19, no. 1, January 2018.

[7] Z. Xia, J. A. Abu Qahouq, and S. Kotru, "Evaluation of permanent magnet distribution schemes for toroid power inductor with increased saturation current using 3D physical models," in *APEC*, pp. 2894-2899, March 2019.

[8] J. A. Abu Qahouq and Z. Xia, "Single-perturbation-cycle online battery impedance spectrum measurement method with closed-loop control of power converter," *IEEE Transactions on Industrial Electronics*, vol. 64, no. 9, pp. 7019-7029, September 2017.

[9] Z. Xia and J. A. Abu Qahouq, "An online battery impedance spectrum measurement method with increased frequency resolution," in *APEC*, pp. 1930-1933, March 2018.

[10] Z. Xia and J. A. Abu Qahouq, "Method for online battery AC impedance spectrum measurement using dc-dc power converter duty-cycle control," in *APEC*, pp. 951-958, March 2017.

[11] Z. Xia and J. A. Abu Qahouq, "High frequency online battery impedance measurement method using voltage and current ripples generated by DC-DC converter," in *APEC*, pp. 1333-1338, March 2020.

[12] S. Rodrigues, N. Munichandraiah, and A. Shukla, "A review of state-of-charge indication of batteries by means of a.c. impedance measurements," *J. Power Sources*, vol. 87, no. 12, pp. 12–20, 2000.

[13] C. Weng, J. Sun, and H. Peng, "Model parametrization and adaptation based on the invariance of support vectors with applications to battery state-of-health monitoring," *IEEE Transactions on Vehicular Technology*, vol. 64, no. 9, pp. 3908-3917, September 2015.

[14] D. Stroe and E. Schaltz, "Lithium-Ion Battery State-of-Health Estimation Using the Incremental Capacity Analysis Technique," *IEEE Transactions on Industry Applications*, vol. 56, no. 1, pp. 678-685, Jan.-Feb. 2020.

[15] Z. Xia, J. A. Abu Qahouq, E. Phillips, and R. Gentry, "A simple and upgradable autonomous battery aging evaluation and test system with capacity fading and AC impedance spectroscopy measurement," in *APEC*, pp. 951-958, March 2017.

[16] Z. Xia and J. A. Abu Qahouq, "State-of-health indication method for li-ion batteries," in *APEC*, pp. 1829-1833, March 2018.

[17] Z. Xia, and J. A. Abu Qahouq, "Adaptive and fast state of health estimation method for lithium-ion batteries using online complex impedance and artificial neural network," in *APEC*, pp. 3361-3365, March 2019.

[18] U. Tröltzsch, O. Kanoun, and H. Tränkler, "Characterizing aging effects of lithium ion batteries by impedance spectroscopy," *Electrochimica acta*, vol. 51, no. 8-9, pp. 1664-1672, January 2006.

[19] Y. Gao, S. Li, and B. Lin, "Economic and Hierarchical Control Multi-Thermal Load for Bidding Ancillary Service," In 2018 *Clemson University Power Systems Conference (PSC)*, pp. 1-5, 2018.

[20] W. Dong, S. Li, and X. Fu, "Artificial Neural Network Control of A Standalone DC Microgrid," In 2018 *Clemson University Power Systems Conference (PSC)*, pp. 1-5, 2018.

[21] D. I. Stroe, M. Swierczynski, A. I. Stan, V. Knap, R. Teodorescu and S. J. Andreasen, "Diagnosis of lithium-ion batteries state-of-health based on electrochemical impedance spectroscopy technique," In *2014 IEEE Energy Conversion Congress and Exposition (ECCE)*, pp. 4576-4582, September 2014.

[22] M. Abouzari, F. Berkemeier, G. Schmitz, and D. Wilmer, "On the physical interpretation of constant phase elements," *Solid State Ionics*, vol. 180, no. 14-16, pp.922-927, June 2009.

[23] Y. Kim, "Refined simplex method for data fitting," In *Astronomical Data Analysis Software and Systems VI, SP Conference Series*, vol. 125, pp. 116-117. 1997.

[24] Gamry Echem Analyst software, Gamry Instruments. [Online]. https://www.gamry.com/assets/Uploads/EchemAnalystSoftwareManual.pdf.

[25] The Interface 5000E™ potentiostat, Gamry Instruments. [Online]. Available: https://www.gamry.com/potentiostats/interface-5000e-potentiostat/.

[26] Tenergy Corp., Fremont, CA Tenergy cylindric Lithium-ion cell 30005-0 datasheet, Tenergy Corp., Fremont, CA.